DEUTSCHES ELEKTRONEN-SYNCHROTRON DESY

DESY SR-77/04
February 1977

Vacuum Ultraviolet Fluorescence under Monochromatic Excitation and Collision Processes in Gaseous Kr and Xe

by

R. Brodmann and G. Zimmerer

II. Institut für Experimentalphysik der Universität Hamburg
and
Deutsches Elektronen-Synchrotron DESY, Hamburg

NOTKESTRASSE 85 · 2 HAMBURG 52

To be sure that your preprints are promptly included in the
HIGH ENERGY PHYSICS INDEX ,
send them to the following address (if possible by air mail) :

DESY
Bibliothek
Notkestraße 85
2 Hamburg 52
Germany

Vacuum ultraviolet fluorescence under monochromatic excitation and collision processes in gaseous Kr and Xe

by

R. Brodmann and G. Zimmerer

II. Institut für Experimentalphysik der Universität Hamburg,

D-2000 Hamburg 50, Germany

and

Deutsches Elektronen-Synchrotron DESY, D-2000 Hamburg 52, Germany

Abstract

The vacuum ultraviolet fluorescence of Kr and Xe and its dependence on gas pressure (10 Torr to 500 Torr) was studied under monochromatic excitation in the vicinity of the first ($^3P_1$) and second ($^1P_1$) resonance states. For excitation purposes, synchrotron radiation from an electron storage ring was used. The exciting light and the fluorescence light were monochromatized at the same time by different monochromators.

Excitatation in the long wavelength tail of the $^3P_1$ states directly results in excited molecules (e.g. $2Kr + \hbar\omega \rightarrow Kr_2^*$). The radiative decay of these molecules results in the first (Kr: 1250 Å, Xe: 1500 Å) and second (Kr: 1470 Å, Xe: 1700 Å) continua. Under resonant $^3P_1$ excitation, molecule formation via three body collisions (e.g. $Kr^* + 2Kr \rightarrow Kr_2^* + Kr$) is established. Kinetic model calculations indicate a population of 0_u^+ and $^{1,3}\Sigma_g^+$ molecular states by three body collisions. The characteristic quantities, $\tau \cdot K$ (lifetime x rate constant) are deduced for different collision processes. Excitation of $^1P_1$ states results in $^1P_1$ emission and the continua. The $^1P_1$ emission contains molecular components. In Xe, it is strongly quenched by collisional interaction between the $^1P_1$ state and a near lying atomic p state. This is established by fluorescence excitation spectroscopy.

1. Introduction

The interest in the vacuum ultraviolet (VUV) fluorescence of gaseous rare gases has grown rapidly since it was demonstrated that these materials are well suited for the development of tunable, high power VUV lasers (Köhler et al 1972, Rhodes 1974, Bradley 1975, Wallace and Kenney-Wallace 1975). Depending on the pressure of the rare gas, the fluorescence spectra consist of either (collision broadened) atomic resonance lines or molecular emission bands. The molecular emission bands are the candidates for laser application.

In an intermediate pressure range (approximately 10 Torr to 500 Torr) different fluorescence bands can be observed simultaneously (Leichner and Ericson 1974, Leichner et al 1976):

(i) The radiative decay of the $ns(3/2)_1$ and $ns'(1/2)_1$ states (n=5 for Kr and n=6 for Xe).

(ii) The radiative decay of vibrationally excited (first continuum) and vibrationally relaxed (second continuum) homonuclear molecules, R_2^* into the repulsive ground state.

Additionally an emission band connected with the $5d(3/2)_1$ state of Xe was observed (Brodmann et al 1976). The emission connected with the $ns'(1/2)_1$ states of Xe seems to have also a molecular contribution (Brodmann et al. 1976).

In nearly all investigations of rare gas fluorescence, "broad band" excitation has been used like high energy electrons (Leichner and Ericson 1974, Leichner et al 1976), protons (Stewart et al 1970) or discharges (Tanaka and Zelikoff 1954, Tanaka 1955, Huffmann et al 1965, Wilkinson 1967). In these experiments the collision kinetics leading to excimer formation and relaxation are severely influenced by free electrons and atomic or molecular ions. Time resolved spectroscopy has been used for the investigation of the complicated kinetics (Leichner and Ericson 1974, Leichner et al 1976). The different processes that funnel highly excited atoms or molecules into the lower radiating states are not understood in detail.

The kinetics in the neutral systems (electrons and ions being absent) may be very important for a better understanding of the relaxation processes. The neutral systems can be investigated under optical excitation of well defined states using a tunable light source in the VUV region. In a recent paper (Brodmann et al 1976) it was demonstrated for the first time that synchrotron radiation of an electron storage ring is well suited for such experiments. Due to the lack of suitable conventional light sources, up to now, optical excitation of rare gas fluorescence was used only for Xe in a small number of experiments (Siek 1968, Freeman et al 1971, Atzmon et al 1974, Fink and Comes 1975). It should be mentioned that a breakthrough has also been achieved using monochromatized synchrotron radiation for excitation purposes in the field of photoluminescence of rare gas solids (see, e.g., Brodmann et al 1974, Ackermann et al 1976).

In this paper we want to report on photoexcited fluorescence of Kr and Xe in an extended pressure range (10 Torr to 500 Torr). The states excited selectively with monochromatic light are the first resonance lines, $ns(3/2)_1(^3P_1)$, the second resonance lines, $ns'(1/2)_1(^1P_1)$, (n=5 for Kr, n=6 for Xe) and molecular states associated with them. Though we use the notation of atomic states we want to point out that already at 10 Torr the influence of rare gas dimers on absorption cannot be neglected (Castex 1974, Freeman et al 1974, Castex and Damany 1974). The pressure dependence of the intensity of the different fluorescence bands enables us to disentangle the processes involved in the collision kinetics and relaxation, provided an appropriate excited state is picked up by monochromatic excitation.

2. Experiment

The experiments were carried out in the new synchrotron radiation laboratory at the electron storage ring DORIS of the Deutsches Elektronen-Synchrotron DESY in Hamburg. The laboratory has been described recently (Koch et al 1976). The synchro-

tron radiation with its intense and continuous spectral distribution was dispersed by a near normal incidence monochromator. The monochromatic light was focused into a LiF gas cell containing either high purity Kr (99.9997 %) or high purity Xe (99.997 %) with a pressure between 10 Torr and 500 Torr. The special design of the gas cell described by Brodmann et al (1976) enabled us to measure simultaneously transmission and fluorescence. The length of the gas cell was 1 cm. The wavelength range of exciting light was limited by the transmission of the LiF gas cell to $\lambda > 1040$ Å. The band pass of exciting light was ~3 Å. At very low pressures, this band pass is much larger than the width of the absorption bands. At higher pressures ($p > 10$ Torr) the widths of the absorption bands of Kr and Xe are comparable or even larger than the band pass of the exciting light.

The fluorescence light was analyzed with a Seya Namioka VUV monochromator attached to the sample chamber. The fluorescing part of the gas cell served as entrance slit of the second monochromator thus giving rise to an upper limit of the resolution of the second monochromator (10 to 30Å). This resolution was sufficient to clearly separate the molecular fluorescence bands. All fluorescence spectra are corrected for the characteristics of the photomultiplier (EMR 541G). They are not corrected for the transmission of the analyzing monochromator because the transmission curve has only a smooth and weak wavelength dependence in the range of interest.

All measurements were carried out at room temperature. More experimental details are given by Brodmann et al (1975).

3. Excitation in the vicinity of the first resonance line

3.1 Fluorescence spectra for different pressures and different excitation wavelengths

In Figs. 1 - 4 the fluorescence spectra of gaseous Kr and Xe are displayed for different pressures and excitation wavelengths. In Fig. 1 (Kr) resonant excitation of the pressure broadened Kr $5s(3/2)_1(^3P_1)$ state was chosen (1236 Å ≙ 10.02 eV). The insert of Fig. 1 shows a transmission curve of Kr in the neighbourhood of the first resonance line at a pressure of 100 Torr. It demonstrates that the resonance line is considerably broadened at higher pressures. The excitation wavelength is indicated in the insert by an arrow. Fig. 2 (Xe) displays the analogous result of Xe (resonant excitation of the Xe $6s(3/2)_1(^3P_1)$ state, excitation wavelength 1470 Å ≙ 8.44 eV).

Both the Ar and Xe curves show the 1st continua (centered around 1240 - 1250 Å (Kr) and 1470 - 1500 Å (Xe)) and the 2nd continua (centered around 1470 Å (Kr) and 1700 Å (Xe)). The peak position at 1720 Å given by Brodmann et al (1976) for the 2nd continuum of Xe was due to the lower resolution (~60Å) obtainable at that time. The curves in Figs.1-4 are normalized to the maxima of the 1st continua for the following reason: at low pressures ($p \lesssim 80$ Torr) total absorption is not reached for the whole band width of exciting light. Therefore it is difficult to normalize the curves to the absorbed intensity of exciting light. Normalization to the absorbed intensity is not necessary if only relative intensities of different fluorescence bands are discussed.

The curves of Figs. 1 and 2 demonstrate a dramatic enhancement of the 2nd continua relative to the 1st continua with increasing pressure. The absolute intensities of the 1st continua decrease. They are no longer detectable at pressures ≳1000 Torr (not shown here). In the pressure range covered by our experiments we are hardly able to discriminate between the resonant emission of the atomic $^3P_1$ state of Kr or Xe atoms (Leichner and Ericson 1974, Leichner et al 1976) and the emission of vibrationally excited dimers of Kr or Xe (1st continua) due to the resolution of 10 - 30 Å of the analyzing monochromator.

Figs. 3 and 4 show the fluorescence curves of Kr and Xe at different pressures, excited in the long wavelength tails of the Kr $5s(3/2)_1$ $(^3P_1)$ and Xe $6s(3/2)_1(^3P_1)$ absorption bands. As excitation wavelengths, 1250 Å (≙ 9.94 eV) for Kr and

1490 Å (≙ 8.33 eV) for Xe were chosen as a compromise between two requirements:

(i) The excitation wavelength should be far away from resonant excitation (at least more than kT).

(ii) The absorption should be large enough to lead to detectable fluorescence.

Similar to Figs. 1 and 2, both continua show up under off-resonant excitation. The relative change of the spectra is much less pronounced than for resonant excitation. The spectral positions of the 1st continua are shifted to longer wavelenghts by about 10 Å (Kr) and 20 Å (Xe), because the excitation wavelength has been shifted, too.

3.2 Pressure dependence of the fluorescence bands

As can be seen from Figs. 1 - 4, the role of the selected excitation wavelength strongly manifests itself in the pressure dependence of the different bands. We discuss the pressure dependence of the relative intensities of the different fluorescence bands for the same reasons as mentioned in section 3.1.

In Fig. 5, the intensity ratios of the 2nd continuum and the 1st continuum (including the non resolved resonant emission) of the Kr fluorescence are plotted as a function of pressure. The intensities of the different bands were obtained by a deconvolution of the measured curves and by integration over the individual contributions. The ratios are given both for resonant excitation of the Kr $^3P_1$ state (1236 Å ≙ 10.02 eV) and off-resonant excitation (1250 Å ≙ 9.94 eV). The corresponding plots for Xe are shown in Fig. 6.

A completely different pressure dependence of the ratios of fluorescence intensities for resonant and off-resonant excitation in the vicinity of the $^3P_1$ states of Kr and Xe is found. Excitation of Kr and Xe in the long wavelength tail of the first resonance line results in an approximately linear increase of the ratio. Resonant excitation results in a complicated pressure dependence. A linear pressure dependence is only reached at rather high pressures. The slope of the linear part of the curve is different from the slope of the "off-resonant" curves.

3.3 Discussion of the results under excitation in the vicinity of the first resonance line

3.3.1 Fluorescence mechanism

It is generally accepted that the 1st and 2nd continua of Kr and Xe are due to the radiative decay of the diatomic molecules Kr_2^* and Xe_2^*. Apart from a shallow van der Waals minimum, the ground states of these molecules are repulsive. The lowest excited states are bound states. The molecules in the lowest excited states ar built up from $ns(3/2)_{1,2}(^3P_{1,2})$ and ^1S_o atoms. Potential curves of Xe_2^* have been published by Mulliken (1970, 1974). In Fig. 7, potential curves of the Xe_2 molecule are shown. The ground state curve is taken from scattering experiments of Farrar et al (1973). The potential curves of the excited states connected with atomic $6s(3/2)_{1,2}$ states are taken from Mulliken (1974). The repulsive potential curves of this group which are dipole forbidden have not been drawn. The solid curve connected with the $6s'(1/2)_1$ atomic state stems from Castex and Damany (1974). The broken potential curves shall indicate that repulsive as well as attractive molecular states connected with higher atomic states exist. Following Mulliken (1970, 1974), the molecular states are classified with Hund's coupling case (c) for large internuclear distances and case (a) for small internuclear distances. In this notations the 1st continuum is due to the radiative decay of the vibrationally excited 1_u and 0_u^+ states to the ground state 0_g^+. The 2nd con-

tinuum stems from the vibrationally relaxed $^{1,3}\Sigma_u^+$ states which decay into the $^1\Sigma_g^+$ ground state. The different contributions to the 2nd continuum of Xe could be identified by life time measurements (Keto et al. 1974). A short component (5.5 ns) was ascribed to $^1\Sigma_u^+$ and a long component (96 ns) to $^3\Sigma_u^+$. Recent time resolved investigations of the fluorescence of gaseous Xe under optical excitation, however, yield radiative lifetimes of the $^3\Sigma_u^+$ state of ≈50 μs (Haaks 1976).

The formation of Kr_2^* and Xe_2^* molecules under optical excitation is discussed in connection with the pressure dependence of the fluorescence intensities.

3.3.2 Pressure dependence under off-resonant excitation

We want to present a simple kinetic model which enables us to explain quantitatively the measured pressure dependence of the ratio of the fluorescence intensities under off-resonant excitation. The model is schematically illustrated in Fig. 8a.

The starting point is the formation of the rare gas molecule, R_2^*, by the absorption process itself.

$$R_2(0_g^+) + h\omega \xrightarrow[1/\tau_0]{\sigma_M} R_2^*(0_u^+) \qquad (1)$$

The molecular type of absorption in the long wavelength tail of the first resonance lines of rare gases has been proved by measuring the pressure dependence of the absorption, $\ln(I_o/I)$ which is proportional to the square of gas pressure (Brodmann 1976). This is in agreement with results of Freeman et al (1974) and Castex and Damany (1974). The $R_2^*(0_u^+)$ state is a vibrationally excited state. It either decays radiatively with a life time τ_0 (1st continuum) or undergoes vibrational relaxation via two body collisions.

$$R_2^*(0_u^+) + R(^1S_o) \xrightarrow{K_2} R_2^*(^1\Sigma_u^+,\ ^3\Sigma_u^+) + R(^1S_o) \qquad (2)$$

The rate constant for this process is K_2. The $^1\Sigma_u^+$, $^3\Sigma_u^+$ states decay radiatively into the repulsive $^1\Sigma_g^+$ ground state (2nd continuum) with the radiative lifetimes $\tau(^1\Sigma_u)$ and $\tau(^3\Sigma_u)$. Here these lifetimes are composed to one single time, τ_u.

$$R_2^*(^{1,3}\Sigma_u^+) \xrightarrow{1/\tau_u} R_2(^1\Sigma_g^+) + h\omega' \qquad (3)$$

Under steady state conditions we obtain from Eqs. (1) to (3) the following result:

$$\frac{I_F(2)}{I_F(1)} = \tau_0 \cdot K_2 \cdot \{R(^1S_o)\} = \tau_0 \cdot K_2 \cdot p \qquad (4)$$

$I_F(2)$ means the intensity of the second continuum, $I_F(1)$ means the intensity of the 1st continuum. $\{R(^1S_o)\}$ is the concentration of ground state atoms which is proportional to the pressure, p. The rules of chemical reaction kinetics have been used. The term which describes the absorption, is canceled by calculating the ratio of the intensities.

The linear dependence of the ratio of fluorescence intensities on pressure under off-resonant excitation is well established by the experimental results shown in Figs. 5 and 6. From the slope of the straight lines in Figs. 5 and 6, values for $\tau_0 \cdot K_2$ can be deduced. We obtain $\tau_0 \cdot K_2 = 6 \times 10^{-19}$ cm^3 for Kr and 5.2×10^{-19} cm^3 for Xe. These values are in good agreement with an estimate of Fink and Comes (1975), $\tau_0 \cdot K_2 = 4 \times 10^{-19}$ cm^3 for vibrational relaxation of Xe_2^* via two body collisions with Kr atoms.

For the determination of K_2 itself, the radiative lifetime τ_0 of the 0_u^+ state must be known. For an estimate of K_2, we adopt the radiative lifetime of the $^1\Sigma_u^+$ state for the 0_u^+ state because these states merge one into each other as a function of internuclear distance. Keto et al. (1974) have measured 5.5 ns for Xe. The Kr value is unknown. With $\tau_0 \approx 6$ ns we obtain $K_2 = 10^{-10}$ cm^3/sec for Kr

and $K_2 = 8.7 \times 10^{-11}$ cm^3/sec for Xe. $K_2 = 2 \times 10^{-11}$ cm^3/sec given by Fink and Comes (1975) is based on an assumption of $\tau_0 = 20$ ns. Our numerical results are listed in Table 1.

3.3.3 Pressure dependence under resonant excitation

We use the model of Fig. 8b for the interpretation of the pressure dependence of the fluorescence intensities under resonant excitation of the $^3P_1$ states. The absorption and the radiative decay of the $^3P_1$ states is described by

$$R(^1S_o) + \hbar\omega \underset{1/\tau_A}{\overset{\sigma_A}{\rightleftharpoons}} R^*(^3P_1) \qquad (5)$$

σ_A is the atomic absorption cross section and τ_A the radiative lifetime of the $^3P_1$ states. τ_A is not identical with the radiative lifetime of an isolated $R^*(^3P_1)$ but increases drastically due to radiation self trapping at higher pressures (Holstein 1951). It has been proved that the pressure dependence of $\ln(I_o/I)$ is linear under resonant excitation in contrast to the case of off-resonant excitation (Brodmann 1976).

Alternatively to the radiative decay of the $R^*(^3P_1)$ atoms, molecules are formed by three body collisions:

$$R^*(^3P_1) + 2R(^1S_o) \xrightarrow{K_3} R_2^*(O_u^+) + R(^1S_o) \qquad (6)$$

The rate constant for this process is K_3. The three body collisions result in vibrationally excited O_u^+ molecules.
According to Fig. 7, the O_u^+ state is not the only candidate which can be reached by three body collisions. We have to include the formation of $^{1,3}\Sigma_g^+$ states which originate from the $^3P_{1,2}$ atomic states. The inclusion of these states into the kinetic has been proposed by Fournier (1975)

$$R^*(^3P_1) + 2R(^1S_o) \xrightarrow{K_3'} R_2^*(^{1,3}\Sigma_g^+) + R(^1S_o) \qquad (7)$$

The $^{1,3}\Sigma_g^+$ states cannot decay radiatively into the ground state $^1\Sigma_g^+$ (parity forbidden). It is assumed that the $^{1,3}\Sigma_g^+$ states decay via infrared radiation into the $^{1,3}\Sigma_u^+$ states and thus directly feed into the 2nd continuum. Under steady state condition therefore the concentration of $^{1,3}\Sigma_g^+$ states is added to the concentration of $^{1,3}\Sigma_u^+$ states.

The radiative decay and the vibrational relaxation of the O_g^+ state are described by Eq. (1) and Eq. (2). The radiative decay of the vibrationally relaxed $^1\Sigma_u^+$, $^3\Sigma_u^+$ states is given by Eq. (3).

Because we are not able to distinguish experimentally between the resonant emission of the $^3P_1$ atoms (Eq. 5) and the 1st continuum (Eq. 1), we now calculate the ratio

$$\frac{I_F(2)}{I_F(1)+I_F(R)} = \frac{\tau_A \cdot K_3' \left(R(^1S_o)\right)^2 + (\tau_A \cdot K_3' + \tau_A \cdot K_3) \cdot \tau_0 \cdot K_2 \left(R(^1S_o)\right)^3}{1 + \tau_0 \cdot K_2 \left(R(^1S_o)\right) + \tau_A \cdot K_3 \left(R(^1S_o)\right)^2} \qquad (8)$$

$I_F(R)$ means the resonant fluorescence (Eq. 5). If we take the values of $\tau_0 \cdot K_2$ from the results under off-resonant excitation, in Eq. (8) only two parameters are unknown, namely $\tau_A \cdot K_3$ and $\tau_A \cdot K_3'$. With the expression given by Eq. (8) we can fit the experimental results of Fig. 5 and Fig. 6. The full, curved lines represent such fits. In this way, values for $\tau_A \cdot K_3$ and $\tau_A \cdot K_3'$ can be deduced. They are listed in Table 1.

The deduction of K_3 and K_3' needs reliable values for τ_A. We take the values for the radiative lifetime of the isolated $^3P_1$ Kr and Xe atoms given by Matthias (1976) (Kr: 5.1 ns, Xe: 3.6 ns). The influence of radiation self-trapping is taken into account according to

$$\tau_A = \frac{1}{g} \cdot \tau \qquad , \qquad g = 0.205\sqrt{\frac{\lambda_o}{D}}$$

These formulae have been given by Holstein (1951). τ means the natural lifetime, λ_0 the wavelength of the resonance line. D is the diameter of the cylindrical gas cell. We obtain τ_A = 5 µs for Kr and τ_A = 3.5 µs for Xe. The resulting K_3 and K_3' values are listed in Table I. The K_3' values are roughly twice the K_3 values. Therefore, the $^{3,1}\Sigma_g^+$ states must play a considerable role in the formation of the molecules.

A good test for the model is a comparison between our results for K_3 and otherwise published data. For Xe, $K_3 = 3.4 \times 10^{-32}$ cm^6/sec (our result) is between the value of 1.7×10^{-32} cm^6/sec (Freeman et al 1971) and 4.5×10^{-32} cm^6/sec (Leichner et al. 1976). For Kr, $K_3 = 8.3 \times 10^{-33}$ cm^6/sec can be deduced from the results of Leichner and Ericson (1974). This value is slightly smaller than our result (2.2×10^{-32} cm^6/sec).

3.3.4 Influence of metastable $^3P_2$ atoms

3.3.4.1 Off-resonant excitation

Excitation in the long wavelength tail of the first resonance line directly leads to the formation of excited molecules Kr_2^*, Xe_2^*. In the decay model presented in Sec. 3.3.2 only two decay channels were taken into account: radiative decay (Eq. 1 and Eq. 3) and vibrational relaxation (Eq. 2). Additionally, two body collisions between a molecule in a high vibrational state and an atom may lead to dissociation of the molecule into a metastable $^3P_2$ atom and a $^1S_0$ atom.

The $^3P_2$ atoms may either lead to quenching or feed back into the radiative channels in a way similar to $^3P_1$ atoms (Sec. 3.3.3). A feed back of $^3P_2$ atoms into the fluorescence bands must give a contribution to the pressure dependence of the ratio of fluorescence bands which clearly differs from linearity. The experimental result does not show such deviations. Therefore the influence of $^3P_2$ atoms seems to be neglegible. However, it cannot be decided whether the rate of dissociation or the feed back is neglegible.

3.3.4.2 Resonant excitation of $^3P_1$ states

In some papers (Turner 1957, Boucique and Mortier 1970, Timpson and Anderson 1970, Atzmon et al. 1974) a collision induced conversion of the atomic $^3P_1$ states to the metastable $^3P_2$ states is reported. Formation of Kr and Xe dimers then starts from the metastable long lived $^3P_2$ states.

We also tried to interprete the results of Sec. 3.2 including the conversion of $^3P_1$ states to $^3P_2$ states by two body collisions. The following results are obtained:

(i) Under the assumption of 100 % conversion of $^3P_1$ atoms to $^3P_2$ atoms (as a limiting case) the measured pressure dependence under resonant excitation of the $^3P_1$ states cannot be fitted, independent of the choice of values for the rate constants.

(ii) If we include molecule formation via the $^3P_2$ state additionally to the channel described by Eq. 6, we are able to fit the measurements. However, it is impossible, to fit the pressure dependence under resonant excitation with the $\tau_0 \cdot K_2$ values obtained from the pressure dependence under off-resonant excitation, independeat of the choice of all other parameters. The $\tau_0 \cdot K_2$ values from a fit including $^3P_2$ states are by a factor of two to three larger than the values obtained under off-resonant excitation.

The simplest models for a consistent interpretation of the pressure dependences of fluorescence ratios under resonant and off-resonant excitation are the models described in Sec. 3.3.2 and Sec. 3.3.3. The conversion of $^3P_1$ to $^3P_2$ states seems to play only a minor role under the experimental conditions of our experiments.

3.3.5 Influence of long radiative lifetimes on the kinetic models

The rate coefficient, K_2, for two body collision deduced from our results (Sec. 3.3.2) sensitively depends on the numerical value of the radiative lifetime of vibrationally excited molecules, $R_2^*(0_u^+)$. Recent direct measurements of the radiative lifetimes (Haaks 1976) yield much larger values ($\tau(0_u^+) \gtrsim 11$ µs) than can be estimated from the results of Keto et al (1974). The numerical values of the radiative lifetimes do not influence the kinetic models themselves but may change the values of the rate constants drastically. At the present time, we are not able to decide between the different values for the radiative lifetime. It may be of interest in this context, that the luminescence band of solid Xe which is very similar to the 2nd continuum of the gas phase, has a component with a radiative lifetime in the µsec range (Hahn et al 1976).

4. Excitation in the vicinity of the second resonance line

4.1 Fluorescence spectra at different pressures

Excitation of Kr and Xe in the vicinity of the $^1P_1$ states in the pressure range covered by our experiments results in three emission bands: the 1st and 2nd continua and a fluorescence connected with the ns' $(1/2)_1$ ($^1P_1$) states (the "$^1P_1$ band").

Fig. 9 presents some fluorescence curves which have been obtained under resonant excitation of the Kr 5s'$(1/2)_1$ ($^1P_1$) state and the Xe 6s'$(1/2)_1$ ($^1P_1$) state. It has been checked carefully that the $^1P_1$ band is not due to stray light of the exciting light. The curves of Fig. 9 have been normalized to the heights of the $^1P_1$ bands.

In both systems, with increasing pressure the 1st and 2nd continua strongly increase compared to the $^1P_1$ band. The $^1P_1$ fluorescence itself decreases and is no longer detectable for pressures ≳1000 Torr (Kr) and ≳100 Torr (Xe). The ratios between the 2nd and 1st continua deviate from the ratios measured under resonant excitation of the $^3P_1$ states.

There is a remarkable difference between both sets of curves of Fig. 9. Relative to the 1st and 2nd continuum, the $^1P_1$ band of Kr is much stronger than the $^1P_1$ band of Xe. In Kr under resonant excitation of the $^1P_1$ state, the $^1P_1$ band plays a dominating role whereas it is weak in Xe.

4.2 Excitation spectra of the fluorescence bands

For Xe, the relative intensities of the three fluorescence bands under $^1P_1$ excitation sensitively depend on the exact excitation wavelength. Within the sensitivity of our experiment this is not the case for Kr. The effect can be demonstrated better in excitation spectra than in fluorescence spectra. Such measurements are shown in Fig. 10a (Kr) and 10b (Xe). They are compared with the corresponding transmission curves of Kr and Xe in the vicinity of $^1P_1$ excitation.

The maxima of the excitation spectra of all the Kr fluorescence bands are resonant with the $^1P_1$ transmission minimum (Fig. 10a). The maxima of the excitation spectra of the 1st and 2nd continuum of Xe also coincide with the $^1P_1$ transmission minimum of Xe. The excitation spectrum of the Xe $^1P_1$ fluorescence clearly has its maximum at the long wavelength molecular tail of the $^1P_1$ absorption band. The shift between the spectral position of the transmission minimum (1296 Å) and the maximum of the excitation spectrum (1300 Å) is clearly larger than the accuracy of the experiment. The difference in energy between

both extrema (≈260 cm^{-1}) is comparable with kT at room temperature (200 cm^{-1}).

4.3 Discussion of the results

4.3.1 Origin of the "$^1P_1$ band"

Within the accuracy of the measurements of Fig. 9, the $^1P_1$ bands of Kr and Xe are resonant with the excitation wavelength. The width of the measured bands is due to the rather poor resolution. Therefore, at first sight, the $^1P_1$ bands seem to be due to the radiative decay of excited atoms (resonance emission). At higher pressures molecular effects have to be taken into account. As can be seen from Fig. 7 there exists a molecular state 0_u^+ with a shallow minimum at rather large internuclear distances. This potential curve is connected to the $6s'(1/2)_1$ state, and the existence of the minimum has been proved by Castex and Damany (1974) for Xe. Transitions from this molecular 0_u^+ state to the 0_g^+ ground state are dipole allowed. Brodmann et al (1976) gave some arguments that the molecular $0_u^+(6s')$ state is involved in the $^1P_1$ band. At higher pressures the molecules should contribute considerably to the $^1P_1$ band. The Stokes shift of the molecular part of the $^1P_1$ band is expected to be small because the depth of the minimum of the 0_u^+ state is expected to be small. Castex and Damany (1974) give a value of ≈1000 cm^{-1} for Xe. The Kr value is unknown.

Striking evidence for the molecular type of $^1P_1$ emission is given by the excitation spectrum of this band (Xe). Fig. 10b clearly shows that the $^1P_1$ band can be excited in the long wavelength, molecular tail of the $6s'(1/2)_1$ absorption.

In analogy to the resonant emission of $^3P_1$ atoms and its overlap with the 1st continuum we interprete the $^1P_1$ band as resonant emission with a molecular contribution. The molecular contribution ($0_u^+ \rightarrow 0_g^+$) increases with increasing pressure and may finally dominate.

4.3.2 Decay channels of the $^1P_1$ states

Excitation of $ns'(1/2)_1(^1P_1)$ states of Kr and Xe not only leads to the $^1P_1$ fluorescence band but also to the 1st and 2nd continua. Deexcitation of the atomic $^1P_1$ states therefore contains two contributions:

(i) Radiative decay (see Sec. 4.3.1)

(ii) Decay processes which lead to a population of the lowest radiative states of Kr, Xe (resonance emission) and the molecules Kr_2^*, Xe_2^* (1st and 2nd continua)

A detailed kinetic model for the population of the fluorescing levels under excitation of the second resonance lines of Kr and Xe seems to be too complicated. The different behaviour of Kr and Xe displayed in the fluorescence and excitation spectra leads to a qualitative description of the relaxation processes.

In Kr we expect two decay channels for deexcitation of the $5s'(1/2)_1(^1P_1)$ atoms:

(i) Radiative decay, dominating at low pressures

(ii) Collision induced molecule formation (Kr_2^{**}).

The first channel is straight forward. The second channel has also been considered by Leichner and Ericson (1974). Part of the Kr_2^{**} may directly feed into the $^1P_1$ band ($0_u^+ \rightarrow 0_g^+$). Part of the Kr_2^{**} molecules may cascade down to lower states and feed into the 1st and 2nd continuum.

Additionally to these decay channels, a collision induced conversion of Kr $5s'(1/2)_1(^1P_1)$ states into Kr $5s'(1/2)_0(^3P_0)$ states cannot be excluded. Because the $^3P_0$ state is a long lived metastable state, its deexcitation is expected to take place via molecular interaction feeding into the 1st and 2nd continuum.

The situation is different in Xe. Besides the radiative decay of the $6s'(1/2)_1$ ($^1P_1$) states and molecule formation we must take into account the role of the $6p(1/2)_1$ state. The energetical distance between the $6s'(1/2)_1$ state and the $6p(1/2)_1$ state is only 84 cm^{-1} (Moore 1949). Therefore the $6s'(1/2)_1$ state can be depopulated efficiently by two body collisions and $6p(1/2)_1$ states are formed. The $6p(1/2)_1$ states can decay radiatively into 6s atomic states. The 6s atomic states give rise to the resonance emission or feed into the 1st and 2nd continuum.

The interesting difference between Kr and Xe is this third decay channel. In Xe, the population of the lowest excited states is possible in the atomic system whereas in Kr the molecular system is essential for the population of the lowest excited states. In Kr, the $5s'(1/2)_1(^1P_1)$ state is separated from the 5p state by 5320 cm^{-1} (Moore 1949) which is too large for collision induced transitions.

The experimental proof for the qualitative model (Xe) is given by the excitation spectra of Fig. 10b. The excitation spectrum of the $^1P_1$ band has its maximum at the long wavelength tail of the $^1P_1$ absorption. The energetical distance between the maximum of the excitation spectrum and the Xe $6p(1/2)_1$ state is $\sim$350 cm^{-1}. This is slightly larger than kT at room temperature ($\sim$200 cm^{-1}). Collisions obviously quench the $^1P_1$ fluorescence as far as the initially excited state (atomic or molecular) is within kT below the 6p state. In Kr, the average kinetic energy of the atoms (at room temperature) is by far too low for the corresponding process. Therefore in Kr the maximum of the excitation spectrum of the $^1P_1$ band coincides with the transmission minimum of the $^1P_1$ absorption.

Acknowledgements

The authors are particularly grateful to Prof. R. Haensel for his stimulating interest in the present work and Dip.-Phys. U. Hahn for his continuous experimental support. They wish to thank also Prof. E. Matthias and Dr. D. Haaks for providing them with unpublished results of lifetime measurements and for helpful discussions. Thanks are due to the BMFT and to DESY for financial support and a scholarship.

References

Ackermann C Brodmann R Hahn U Suzuki A and Zimmerer G 1976 phys. stat. sol. (b) 74, 579-590

Atzmon R Chesnovsky O Raz B and Jortner J 1974 Chem.Phys.Letters 29, 310-313

Boucique R and Mortier P 1970 J.Phys. D3, 1905-1911

Bradley D J 1975 in Lasers in Physical Chemistry and Biophysics (Amsterdam: Elsevier)

Brodmann R Haensel R Hahn U Nielsen U and Zimmerer G 1974 Chem. Phys. Letters 29, 250-252

Brodmann R 1976 thesis Hamburg

Brodmann R Hahn U and Zimmerer G 1976 Chem.Phys.Letters 41, 160-164

Castex M C 1974 Chem.Phys. 5, 448-455

Castex M C and Damany N 1974 Chem.Phys.Letters 24, 437-440

Farrar J M Schafer T P and Lee Y T 1973 Transport Phenomena: AIP Conference Proceedings No. 11 (New York: AIP)

Fink E H and Comes F J 1975 Chem.Phys.Letters 39, 267-272

Fournier G R 1975 Optics Communic. 13, 385-389

Freeman C G McEwan M J Claridge R F C and Philips L F 1971 Chem.Phys.Letters 10, 530-532

Freeman D E Yoshino K and Tanaka Y 1974 J.Chem.Phys. 61, 4880-4889

Haaks D 1976 private communication

Hahn U Schwentner N and Zimmerer G 1976 to be published

Holstein T 1951 Phys.Rev. 83, 1159-1168

Huffman R E Larrabee J C and Tanaka Y 1965 Appl. Optics 4, 1581-1588

Koch E E Kunz C and Weiner E 1976 Optik 45, 385-410

Koehler H A Ferderber L J Redhead D L and Ebert P J 1972 Appl.Phys.Lett. 21, 198-200

Keto J W Gleason R E and Walters G K 1974 Phys.Rev.Letters 33, 1365-1368

Leichner P K and Ericson R J 1974 Phys.Rev. A9, 251-259

Leichner P K Palmer K F Cook J D and Thienemann M 1976 Phys.Rev. A13, 1787-1792

Matthias E 1976 private communication

Moore C E 1949 in Atomic Energy Levels, Circular No. 467 of the National Bureau of Standards (Washington)

Mulliken R S 1970 J.Chem.Phys. 52, 5170-5180

Mulliken R S 1974 Rad.Res. 59, 357-362

Rhodes C K 1974 IEEE J. Quantum Electron. QE10, 153-174

Siek L W 1968 J.Phys.Chem. 9, 3129-3133

Stewart T E Hurst G S Bortner T E Palms J E Martin F W and Weidner H L 1970 JOSA 60, 1290-1296

Tanaka Y and Zelikoff M 1954 Phys.Rev. 93, 933-

Timpson R R and Anderson J M 1970 Can.J.Phys. 48, 1817-1829

Turner R 1967 Phys.Rev. A158, 121-129

Wallace S C and Kenney-Wallace G A 1975 Int.J.Radiat.Chem. 7, 345-362

Wilkinson P G 1967 Can.J. of Phys. 45, 1715-1727

Table I

	$\tau_o \cdot K_2$ (cm^3)	K_2 (cm^3/sec)	$\tau_A \cdot K_3$ (cm^6)	$\tau_A \cdot K_3'$ (cm^6)	K_3 (cm^6/sec)	K_3' (cm^6/sec)	K_3 ($^3P_1$) (cm^6/sec)
Kr	6×10^{-19}	10^{-10}	1.1×10^{-37}	2.2×10^{-37}	2.2×10^{-32}	4.4×10^{-32}	8.3×10^{-33} (a)
Xe	5.2×10^{-19}	8.7×10^{-11}	1.2×10^{-37}	2.15×10^{-37}	3.4×10^{-32}	6×10^{-32}	1.7×10^{-32} (b) 4.5×10^{-32} (c)
remarks	$\tau_o \gtrsim 6$ ns estimated		$\tau_A = 5$ ns (Kr) $\tau_A = 3.5$ ns (Xe) estimated				literature values

(a) Leichner and Ericson (1974)

(b) Freeman et al. (1971)

(c) Leichner et al. (1976)

Rate constants for two body collisions, K_2, (vibrational relaxation of Kr_2^*, Xe_2^* molecules) and three body collisions, K_3, (formation of Kr_2^* and Xe_2^* molecules) deduced from model calculations. For comparison literature values are included as far as available.

Figure captions

Fig. 1 Fluorescence spectra of gaseous Kr under resonant excitation of the Kr $5s(3/2)_1(^3P_1)$ state at different pressures. The insert shows a transmission curve of Kr at 100 Torr around the first resonance line. The excitation wavelength for the fluorescence curves is marked by an arrow.

Fig. 2 Fluorescence spectra of gaseous Xe under resonant excitation of the Xe $6s(3/2)_1(^3P_1)$ state at different pressures. The insert shows a transmission curve of Xe at 100 Torr around the first resonance line. The excitation wavelength for the fluorescence curves is marked by an arrow.

Fig. 3 Fluorescence spectra of gaseous Kr under off-resonant excitation of the Kr $5s(3/2)_1(^3P_1)$ state at different pressures. The arrow in the insert indicates the excitation wavelength for the fluorescence bands.

Fig. 4 Fluorescence spectra of gaseous Xe under off-resonant excitation of the Xe $6s(3/2)_1(^3P_1)$ state at different pressures. The arrow in the insert indicates the excitation wavelength for the fluorescence bands.

Fig. 5 Pressure dependence of the ratio of fluorescence intensities of the 1st (including resonance emission) and 2nd continuum of Kr under off-resonant excitation (○) and resonant excitation (●) of the first resonance line. The full curves are results of model calculations.

Fig. 6 Pressure dependence of the ratio of fluorescence intensities of the 1st (including resonance emission) and 2nd continuum of Xe under off-resonant excitation (Δ) and resonant excitation (o) of the first resonance line. The full curves are results of model calculations.

Fig. 7 Potential curves of Xe_2 molecules as a function of internuclear distance. Details and references are given in the text.

Fig. 8 Schematic representation of the kinetic models used for the interpretation of the pressure dependence of fluorescence intensity ratios a) under off-resonant excitation, b) under resonant excitation of the first resonance line. ⇝ means radiative decay, —· means collisions. The collision partners, rate constants and time constants are indicated in the diagrams.

Fig. 9 Fluorescence spectra of a) gaseous Kr and b) gaseous Xe under resonant excitation of the $5s'(1/2)_1$ (Kr) and $6s'(1/2)_1$ (Xe) $^1P_1$ states at different pressures. The wavelengths of the exciting light are indicated by arrows.

Fig. 10 Excitation spectra of all investigated fluorescence bands of a) Kr and b) Xe in the vicinity of $5s'(1/2)_1$ (Kr) and $6s'(1/2)_1$ (Xe) excitation. In an excitation spectrum, the fluorescence intensity of one single fluorescence band is measured as a function of excitation wavelength. At the top, transmission curves are given.

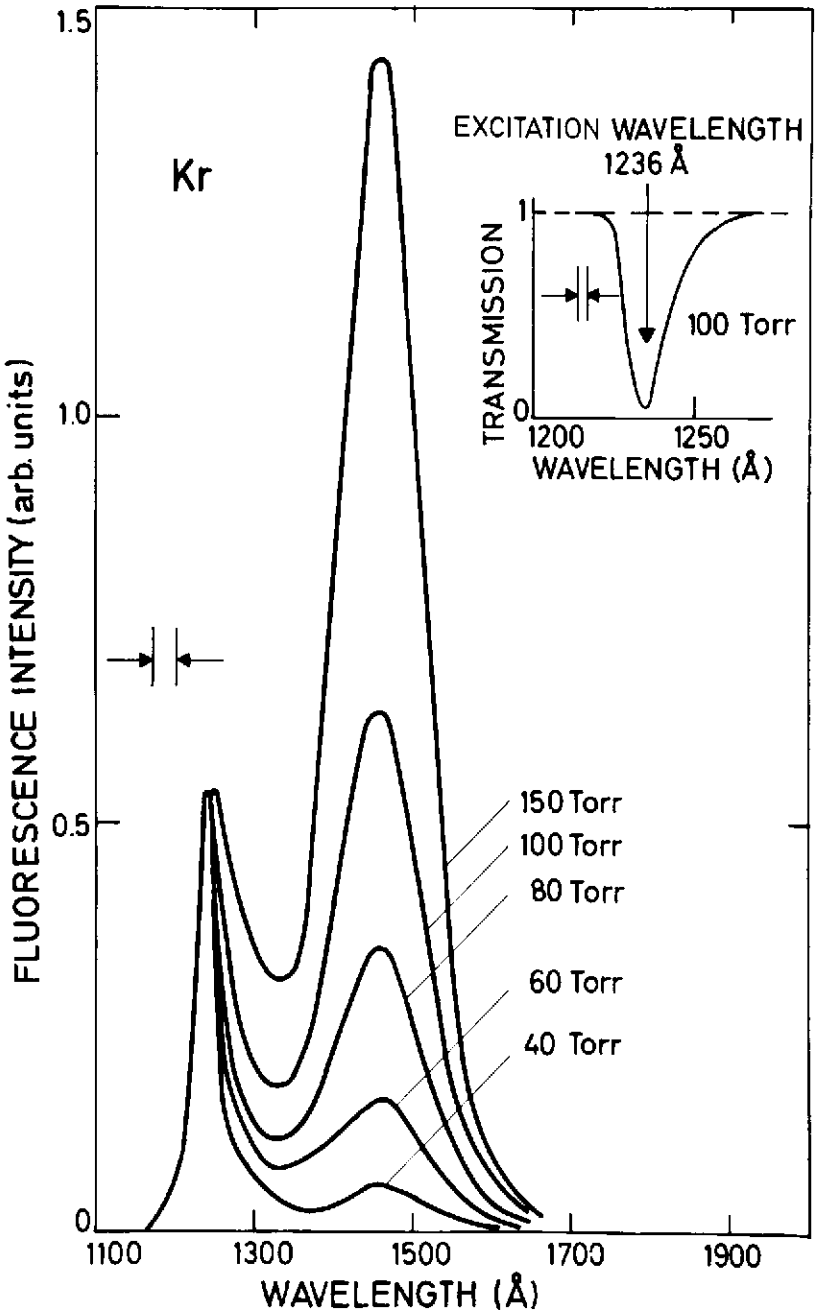

Fig. 1

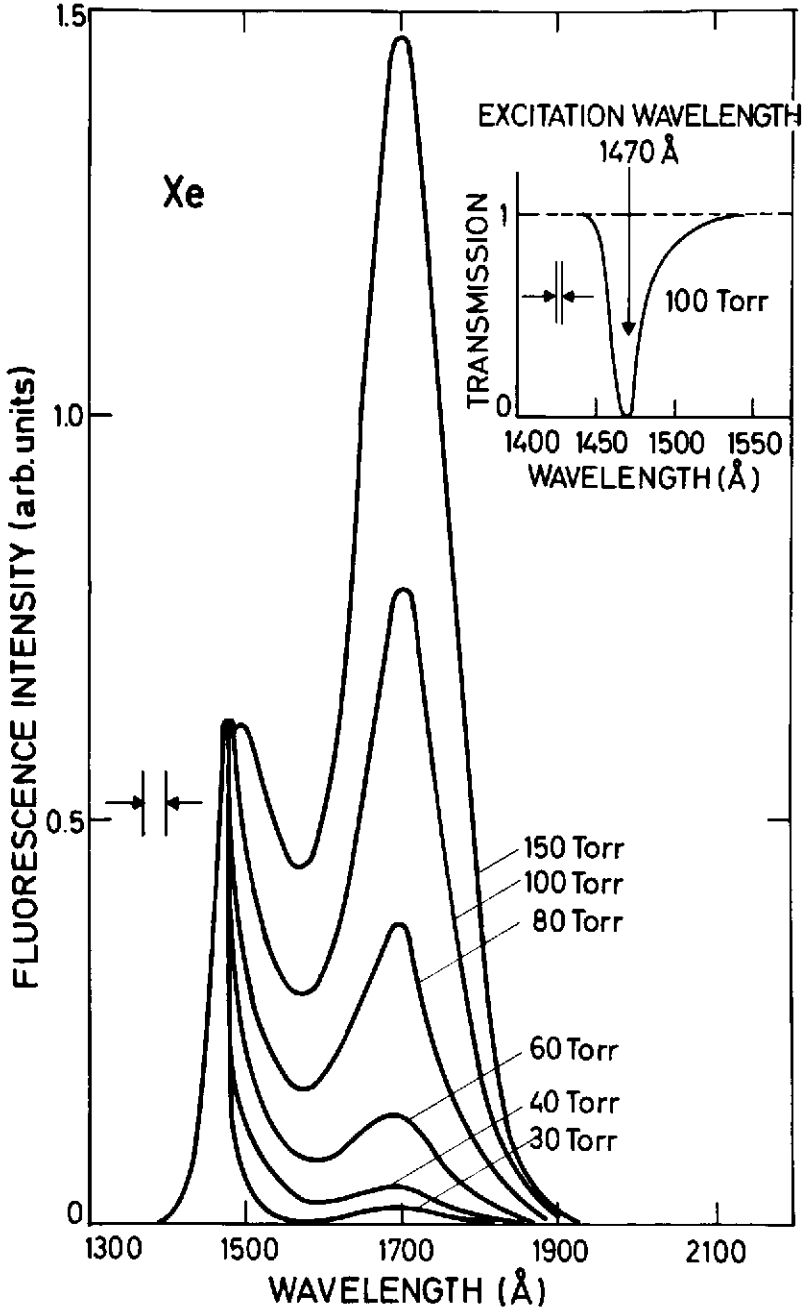
Xe
EXCITATION WAVELENGTH
1470 Å
TRANSMISSION
100 Torr
1400 1450 1500 1550
WAVELENGTH (Å)
FLUORESCENCE INTENSITY (arb.units)
150 Torr
100 Torr
80 Torr
60 Torr
40 Torr
30 Torr
1300 1500 1700 1900 2100
WAVELENGTH (Å)

Fig. 2

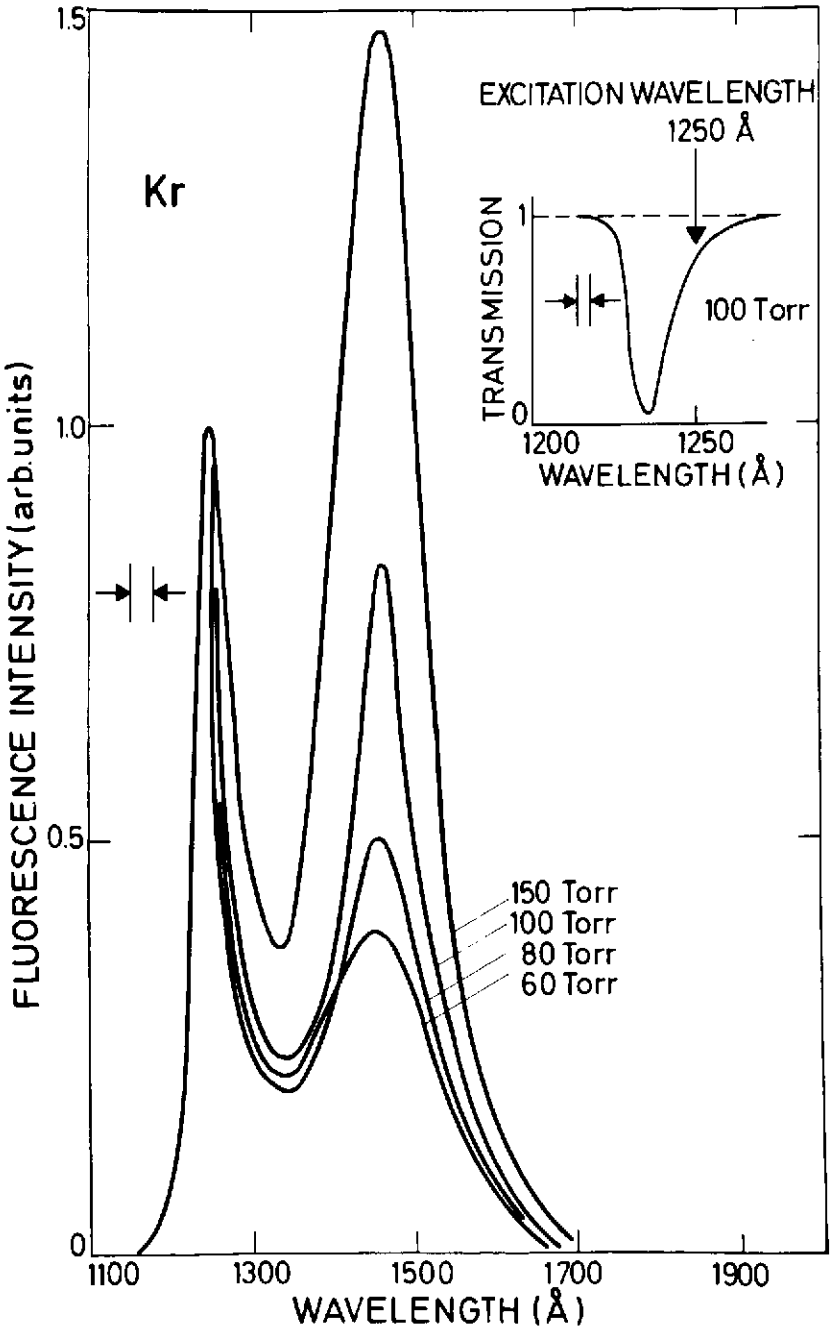
Kr
EXCITATION WAVELENGTH
1250 Å
TRANSMISSION
100 Torr
1200 1250
WAVELENGTH (Å)
FLUORESCENCE INTENSITY (arb.units)
150 Torr
100 Torr
80 Torr
60 Torr
1100 1300 1500 1700 1900
WAVELENGTH (Å)

Fig. 3

DESY

25910

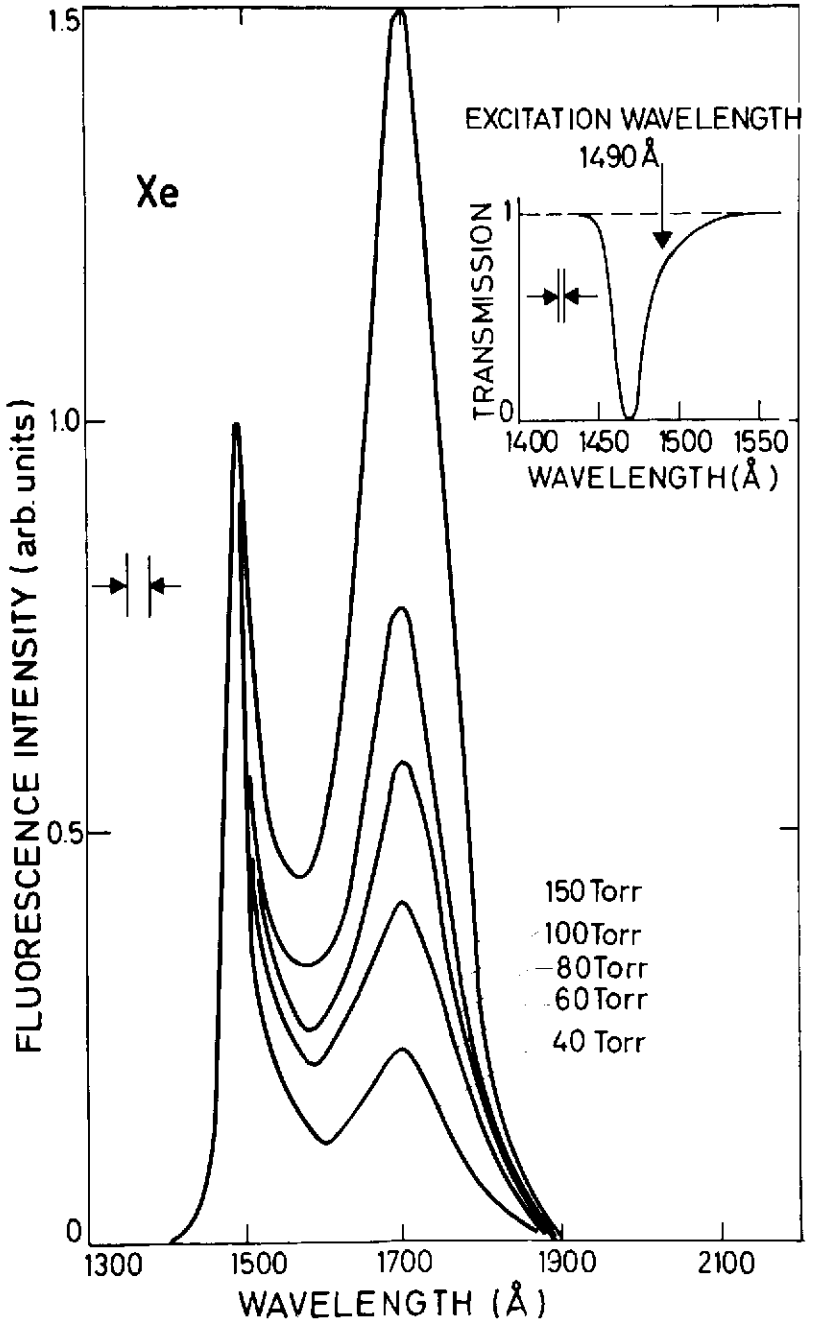

Fig. 4

DESY

25912

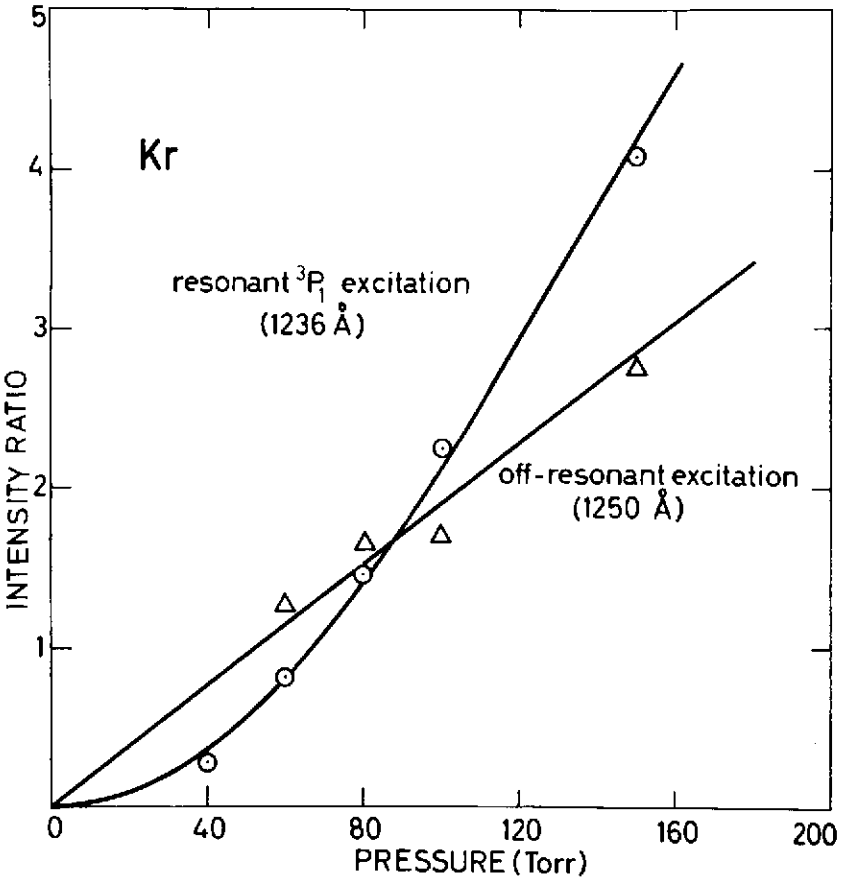

Fig. 5

DESY

25907

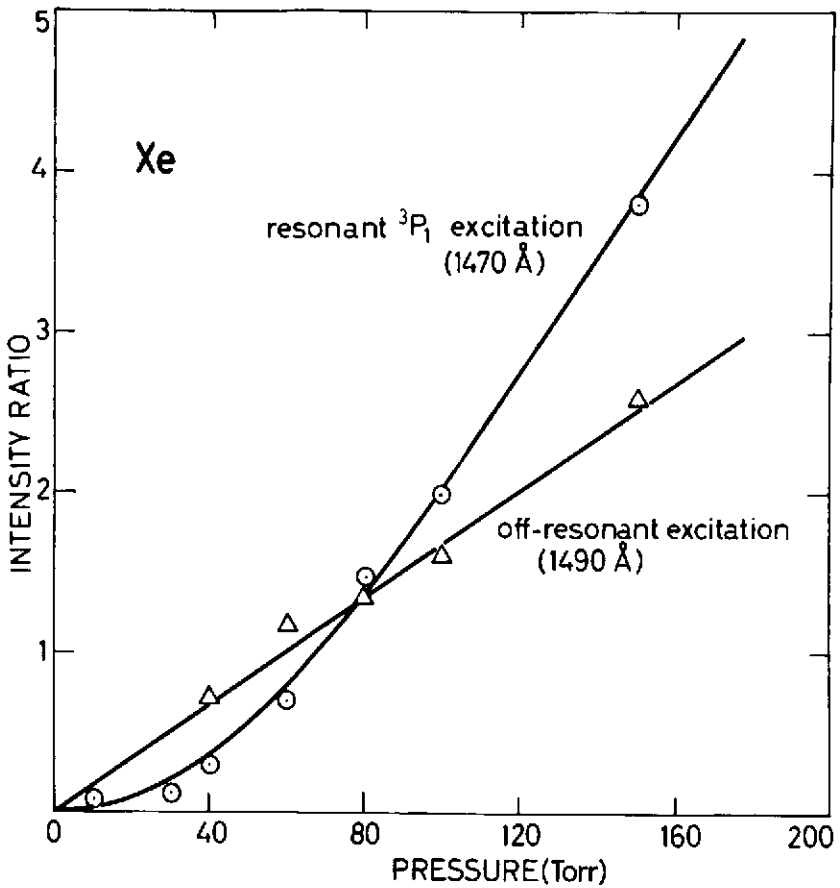

Fig. 6

DESY

25904

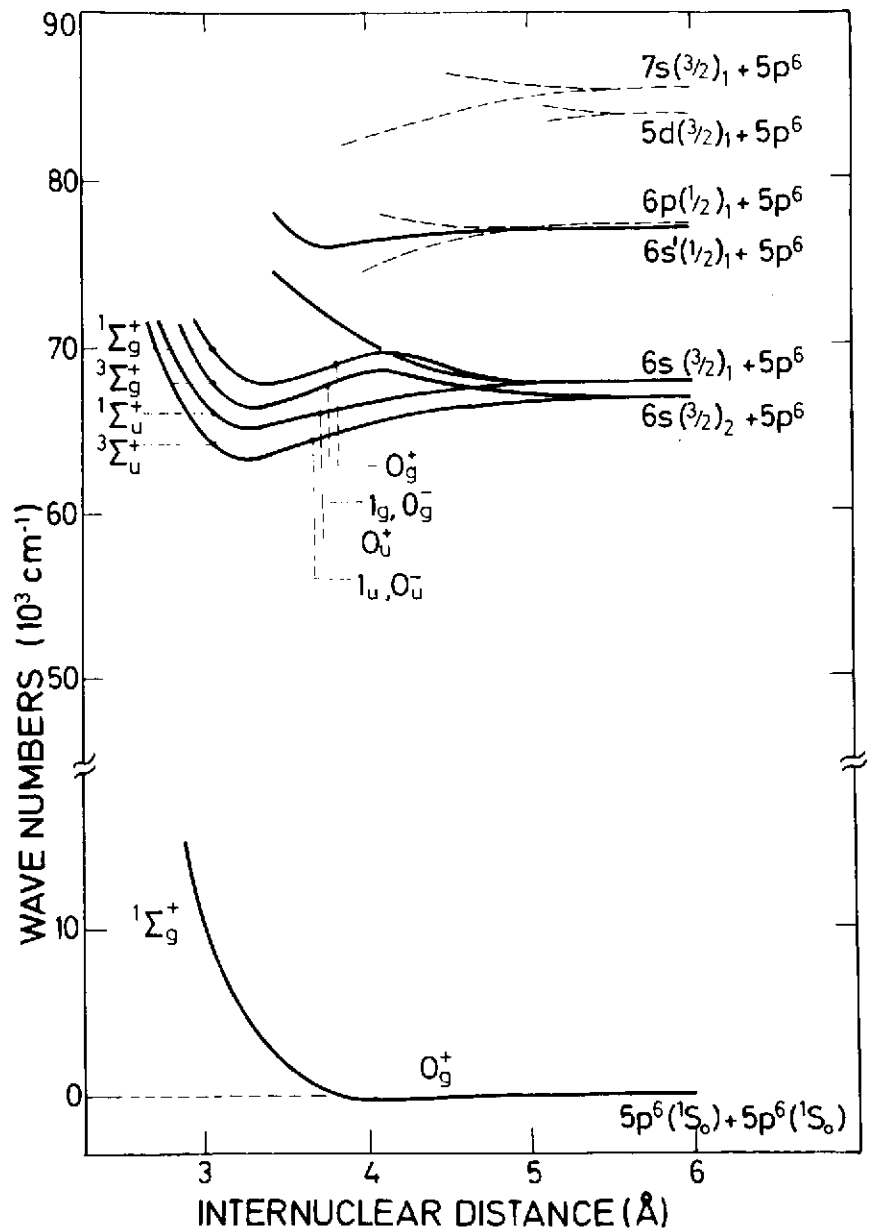

Fig. 7

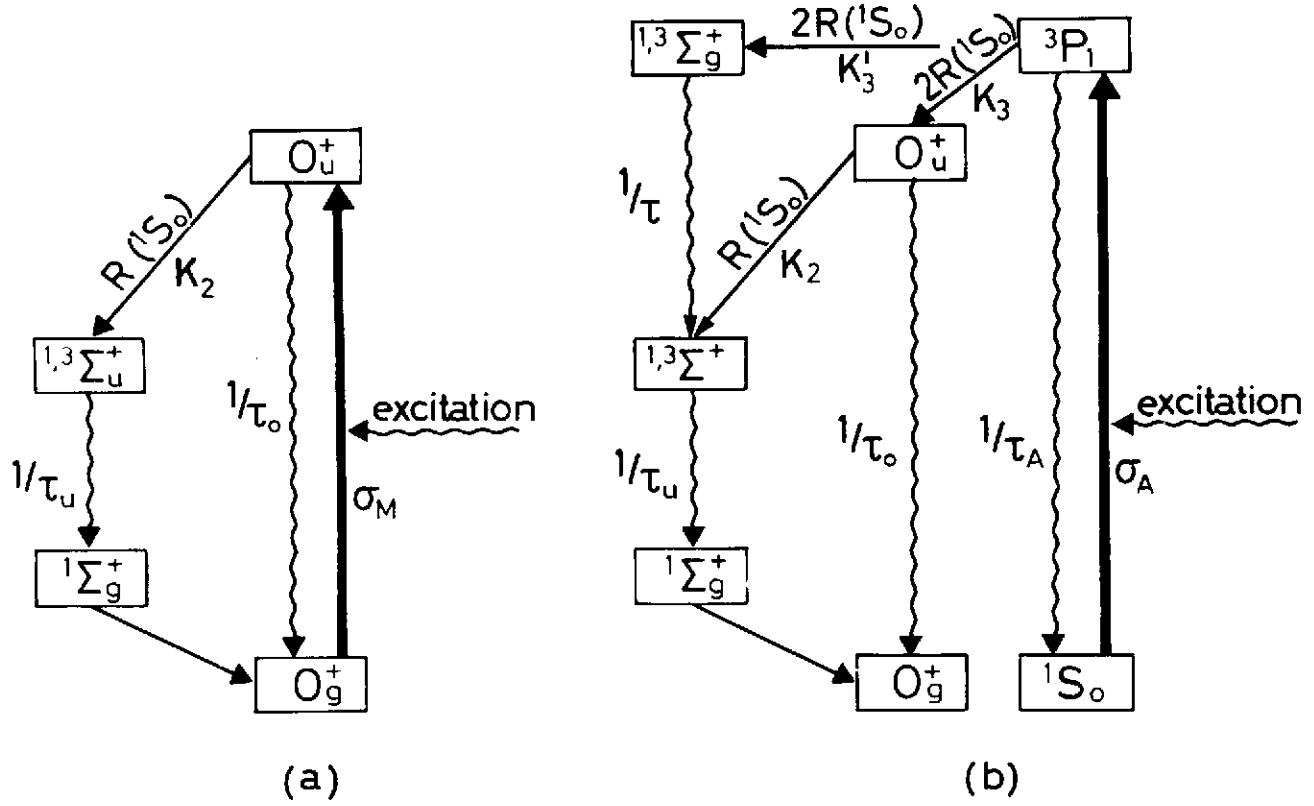
O_u^+
$R(^1S_o)$
K_2
$^{1,3}\Sigma_u^+$
$1/\tau_o$
excitation
$1/\tau_u$
σ_M
$^1\Sigma_g^+$
O_g^+
(a)
$^{1,3}\Sigma_g^+$
$2R(^1S_o)$
K_3'
$^3P_1$
$2R(^1S_o)$
K_3
O_u^+
$1/\tau$
$R(^1S_o)$
K_2
$^{1,3}\Sigma^+$
excitation
$1/\tau_o$
$1/\tau_A$
$1/\tau_u$
σ_A
$^1\Sigma_g^+$
O_g^+
^1S_o
(b)

Fig. 8

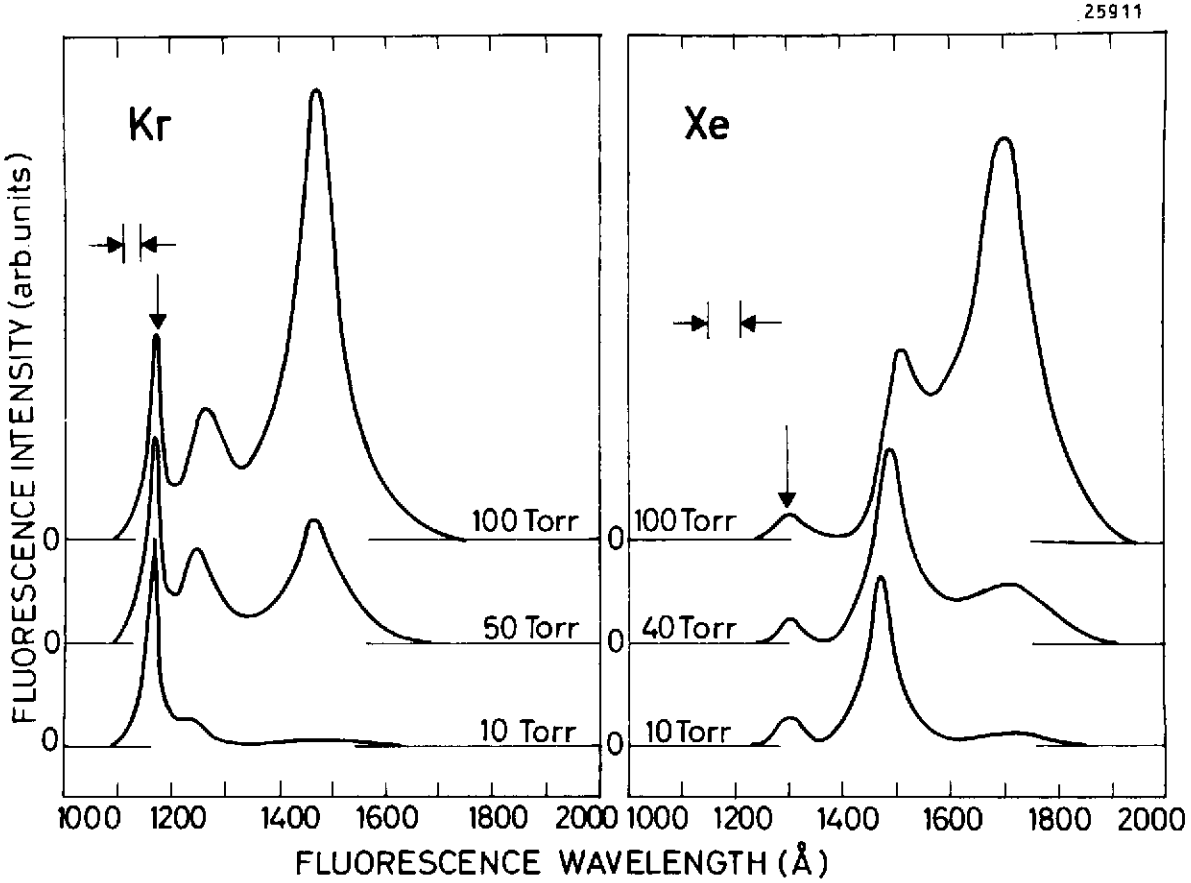
Kr
Xe
100 Torr
50 Torr
10 Torr
100 Torr
40 Torr
10 Torr
0
0
0
0
0
0
FLUORESCENCE INTENSITY (arb.units)
1000 1200 1400 1600 1800 2000
1000 1200 1400 1600 1800 2000
FLUORESCENCE WAVELENGTH (Å)

Fig. 9

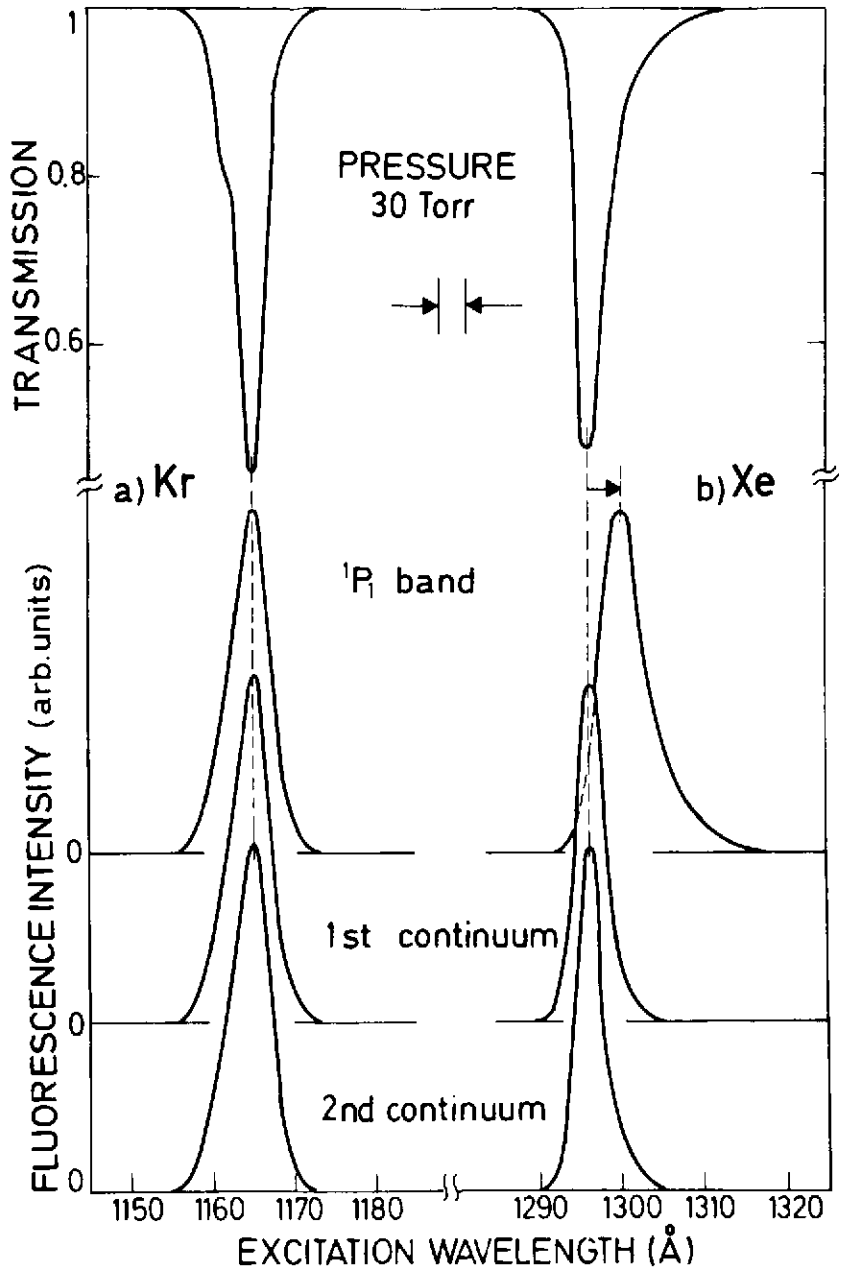
TRANSMISSION
1
0.8
0.6
PRESSURE
30 Torr
a) Kr
b) Xe
FLUORESCENCE INTENSITY (arb.units)
$^1P_1$ band
1st continuum
2nd continuum
0
0
0
1150
1160
1170
1180
1290
1300
1310
1320
EXCITATION WAVELENGTH (Å)

Fig. 10